

1 ***PhenoImage: an open-source GUI for plant image analysis***

2 Feiyu Zhu^{1*}, Manny Saluja^{2*}, Jaspinder Singh^{2*}, Puneet Paul^{2*}, Scott E. Sattler^{2,3}, Paul
3 Staswick², Harkamal Walia², Hongfeng Yu^{1†}

4
5 ¹Department of Computer Science and Engineering, University of Nebraska-Lincoln, USA

6 ²Department of Agronomy and Horticulture, University of Nebraska-Lincoln, USA

7 ³Wheat, Sorghum and Forage Research Unit, USDA-ARS, Lincoln, NE, USA

8

9 * equal contribution

10 †Corresponding author: HY: hfyu@unl.edu

11

12 Others:

13 FZ: feiyuzhu520@gmail.com

14 MS: saluja.manny12@gmail.com

15 JS: jaspinderjawandha75@gmail.com

16 PP: puneet6288@gmail.com

17 SS: scott.sattler@usda.gov

18 PS: pstaswick1@unl.edu

19 HW: hwalia2@unl.edu

20

21 Date of submission: September 1, 2020

22 Number of Tables: 1, Number of Figures: 9, Number of Supplementary Figures: 2, Number of

23 Supplementary Tables: 3, Word count: 4327

24 **Highlight**

25 *PhenoImage* is an open-source application designed for analyzing images derived from high-
26 throughput phenotyping.

27

28 **Abstract**

29 High-throughput genotyping coupled with molecular breeding approaches has dramatically
30 accelerated crop improvement programs. More recently, improved plant phenotyping methods
31 have led to a shift from manual measurements to automated platforms with increased scalability
32 and resolution. Considerable effort has also gone into the development of large-scale
33 downstream processing of the imaging datasets derived from high-throughput phenotyping
34 (HTP) platforms. However, most available tools require some programming skills. We developed
35 *PhenoImage* – an open-source GUI based cross-platform solution for HTP image processing
36 with the aim to make image analysis accessible to users with either little or no programming
37 skills. The open-source nature provides the possibility to extend its usability to meet user-
38 specific requirements. The availability of multiple functions and filtering parameters provides
39 flexibility to analyze images from a wide variety of plant species and platforms. *PhenoImage* can
40 be run on a personal computer as well as on high-performance computing clusters. To test the
41 efficacy of the application, we analyzed the LemnaTec Imaging system derived RGB and
42 fluorescence shoot images from two plant species: sorghum and wheat differing in their physical
43 attributes. In the study, we discuss the development, implementation, and working of the
44 *PhenoImage*.

45

46 **Keywords:** high-throughput phenotyping, image processing, plant phenotyping, RGB images,
47 fluorescence images, sorghum, wheat

48

49 **Introduction**

50 In the genomics and post-genomics era, technological advances in sequencing platforms have
51 paved the way for high throughput genotyping (Jackson *et al.*, 2011; Furbank and Tester, 2011).
52 These developments coupled with molecular breeding approaches have enhanced the genetic
53 understanding of plants, which has dramatically progressed the crop-improvement efforts
54 (Moose and Mumm, 2008; Varshney *et al.*, 2009; Tester and Langridge, 2010). However, precise
55 and efficient phenotyping has been a challenge (Furbank and Tester, 2011). To tackle this
56 problem, plant phenotyping technologies have achieved a huge leap in recent times; the shift
57 from laborious and error-prone manual measurements towards automation (Fiorani and Schurr,
58 2013; Gong and He, 2014). Automated imaging-based platforms have tremendously enhanced
59 our ability to record a plant's physical and physiological attributes in a non-invasive manner.
60 Despite these advances, phenotyping technologies still trail developments on the genomics front,
61 especially the rate at which the phenotypic data is generated (Houle *et al.*, 2010; Furbank and
62 Tester, 2011; Minervini *et al.*, 2015; Gehan *et al.*, 2017). The major limit is not the ever-evolving
63 sophisticated instrumentation for image capturing but with the downstream processing of large-
64 scale phenotypic data, which is not easily accessible to many plant biologists.

65 High-throughput (HTP) imaging platform refers to the accurate acquisition and analysis
66 of multidimensional traits at the individual plant level in context of this work (Yang *et al.*, 2020).
67 To no surprise, these platforms generate a diversity of images corresponding to different spectra
68 of light such as RGB, near-infrared, fluorescence, and hyperspectral. Thus, terabytes of digital
69 information can be routinely generated through an imaging experiment. Currently, the website:
70 www.plant-image-analysis.org, documents 179 image software tools (Lobet *et al.*, 2013).
71 Availability and usage of some of these tools are being restricted and adheres to proprietary
72 rights, for instance LemnaGrid-Scanalyzer3D by LemnaTec GmbH, Germany. On the other
73 hand, several open-source tools designed for specific applications, ranging from cell to whole
74 canopy analysis, are readily accessible in the public domain (Lobet *et al.*, 2013). In addition to
75 their broader functionalities these have also opened new avenues to integrate third-party
76 algorithms. Examples include HTPPheno (developed as a plugin for ImageJ) (Hartmann *et al.*,
77 2011), Plant Computer Vision or Plant CV (a community-based toolkit for plant phenotyping
78 analysis) (Fahlgren *et al.*, 2015; Gehan *et al.*, 2017), Integrated Image Platform or IAP (Klukas
79 *et al.*, 2014), Image Harvest (Knecht *et al.*, 2016). Despite their power and flexibility, these tools

80 may require some proficiency with programming language as a pre-requisite to process large-scale
81 datasets. This is a challenge for many biologists with limited or no coding skills.

82 The availability of several affordable automated and semi-automated phenotyping
83 platforms has increased their usage to score the traits of interest (Klukas *et al.*, 2014; Li *et al.*,
84 2014). Keeping this view in mind, we developed *PhenoImage* – an open-source, GUI-based
85 cross-platform solution for large-scale data processing that is not only convenient to use but
86 highly precise and effective at the same time. The intuitive nature of the application will allow
87 plant scientists with little or no knowledge of programming language to process phenotypic
88 dataset on their personal computers. In addition, the application can facilitate parallel processing
89 of large-scale image data on high-performance computing clusters. To test the efficacy of the
90 application, we analyzed the LemnaTec Imaging system-derived RGB and fluorescence images
91 from sorghum and wheat, which differ in their physical attributes. The availability of multiple
92 functions and filtering parameters provides flexibility to analyze a wide variety of plant species.
93 Images acquired from other phenotyping platforms or handheld devices can also be processed
94 using *PhenoImage*.

95

96 **Materials and Methods**

97 ***PhenoImage* Workflow**

98 *PhenoImage* is a MATLAB-based application i.e. compatible with multiple operating systems.
99 The software is available in two versions, a regular version that requires MATLAB license and a
100 standalone version that uses ‘MATLAB Compiler Runtime’ and does not necessarily require
101 MATLAB license for its operation. Both versions can be downloaded from:
102 <http://wrchr.org/phenolib/phenoinage>. The same graphical user interface (GUI) application can
103 support image data processing on a single central processing unit (CPU) as well as parallel
104 processing on High Performance Computing (HPC) clusters.

105

106 **Software Development and Implementation**

107 The GUI for high throughput image analysis is based on MATLAB. The summary of image
108 processing workflow of *PhenoImage* includes: (i) file loading, (ii and iii) image cropping and
109 filtering, (iv) digital trait extraction using specific functions (based on the user’s requirement),

110 (v) followed by image processing either on a local machine or HPC clusters (Fig. 1). We have
111 provided a step-by-step guide to use *PhenoImage* (see *PhenoImage* Guide Document).

112

113 **File loading**

114 The image files can be loaded by specifying regular expressions in '*Path*' using the following
115 format: "FOLDER NAME*.png". This should allow the loading of all images under the
116 respective folder. The application is compatible with widely used image formats such as
117 *jpg*, *png*, and *tiff*. The spinner can be used to change the '*Original Image*' that is currently
118 displayed (Fig. 2).

119 The visible images (RGB) of plants can be obtained using any system such as LemmaTec
120 or using standard digital cameras. If analyzing images using standard digital cameras, the user
121 must ensure constant focal distance to have similar scale for all the images corresponding to the
122 same batch to facilitate precise comparison.

123

124 **Selection of Region of Interest (ROI) and Image Filtering**

125 For selecting ROI, the user can either crop the image interactively by dragging a marquee tool
126 over the image or by typing the position of the ROI using this format, [X_min, Y_min, Width,
127 Height], where X_min, Y_min is the coordinate of the upper-left corner, and Width and Height
128 correspond to the size of the ROI. The ROI selected is fixed for the image analysis of the
129 respective folder. Thus, it is recommended that the user selects a relatively larger ROI. This is
130 important especially during the analysis of plant growth dynamics in a temporal manner where
131 plants tend to increase in size.

132 Next, image segmentation separates plant pixels from the background. For segmentation,
133 a logical expression can be specified in '*Filter*' (Fig. 2). The application supports (1) red, green,
134 and blue (*RGB*), (2) hue, saturation, and value (*HSV*), and (3) *Lab* color spaces, which provide
135 flexibility to the user to optimally segment the RGB images. Any combination of arithmetic and
136 logical operation can be used to segment the plant. In terms of setting the filter, '&' means
137 logical *AND*, '|' means logical *OR*. For example, 'r<200 & g< 150' means finding pixels that
138 have red values less than 200 and green values less than 150. The '*Processed Image*' will be
139 displayed after clicking '*Test*' button (Fig. 2).

140 If the user is unsure about predefining the filter, then the ‘*Segmentation*’ feature can be
141 utilized (Zhu *et al.*, 2020). For this, click on ‘*Foreground*’ and a new pop-up window having the
142 original image appears. The user can select the zoom-in option from the task bar menu to enlarge
143 the area of interest (i.e., plant tissue in this case). Once the area is zoomed in, the user can
144 deselect the zoom in option and scribble on the enlarged area of interest with a red mark (Fig. 3).
145 Next, background (i.e., pot, pot stand, plant background, etc.) is to be selected by clicking the
146 ‘*Background*’ button and scribble on the background using a green mark. Afterwards, the user
147 can click the ‘*Segment*’ button to initiate the segmentation or subtraction of plant pixels from the
148 background (Fig. 3). We empirically segment the plant by finding plant pixels where the
149 difference to the mean of selected foreground is less than 60. Implementation of the ‘*Segment*’
150 function may take a few additional seconds. After segmentation, the ‘*Processed Image*’ will
151 show pixels corresponding only to the plant and the histograms corresponding only to the plant
152 region will be displayed in ‘*Channel 1, 2, and 3*’. The range of the histogram for each channel
153 can be used to define ‘*Filter*’ parameters. The ‘*Segmentation*’ feature is helpful to define filter
154 parameters in a similar manner for both RGB and fluorescence images; however, histogram
155 values for only the red channel need to be considered for setting the filter in the case of
156 fluorescence images.

157

158 **Defining Functions for Plant Trait Analysis**

159 For digital trait extraction, the user can select functions from a dialog window by clicking
160 ‘*Functions*’, where any user defined functions can be selected. The selected functions will be
161 listed in the text region and will take the segmented image as input to extract digital traits. Some
162 of the commonly used functions are defined below:

163

164 *Pixel Count*

165 After segmentation, only the pixels corresponding to the plant are kept, while pixels
166 corresponding to other objects in the image are set to black. The tool counts the number of pixels
167 that belong to the plant in the ROI.

168

169 *Pixel Intensity*

170 Pixel Intensity refers to the sum of the intensities of pixels in an image. As there are three
171 channels, red, green, and blue, we calculate the pixel sum of each of the R, G, and B channels
172 separately.

173

174 *Dimension*

175 To define the dimensions (width and height), firstly a bounding box, which based on the
176 segmented pixels and encloses all pixels of the plant, is found (Fig. 4). Then, the width and
177 height of the bounding box are used to define the dimensions of the plant.

178

179 *Convex Area*

180 Convex Area is a feature i.e. related to the shape of the plant. The convex area is the area of the
181 convex hull. The convex hull is the smallest convex polygon enclosing all the pixels of the plant
182 (Fig. 4).

183

184 *Image Skeleton*

185 We find the skeleton of the plant pixels using a skeletonization algorithm (Abeyasinghe *et al.*,
186 2008). The skeleton of the plant approximates the center lines of the stem and the leaves. Then,
187 the number of pixels in the skeleton is obtained (Fig. 4).

188

189 *Image moment*

190 Image moments can be used to evaluate the shape of the plant (Hu, 1962). We evaluate the
191 image moment of the binary image or the segmented plant image. For the binary image, the plant
192 pixel is considered as 1, and pixels of other objects in the image (e.g., pot, pot-holder, and
193 background) is considered as 0. The moment of the binary image is only dependent on the
194 positions of the pixels. The fourth-order central image moment (μ_{22}) is evaluated for the binary
195 image in default. The user can easily modify the function to obtain image moments of other
196 orders.

197

198 **Execution on a Local Machine**

199 *Image Processing and Results collection*

200 The batch image processing can be initiated by clicking ‘Execute’ (Fig. 2). The ‘light bulb’
201 located on the right side indicates the status of processing. For instance, the light bulb turns red
202 as images are being processed and will turn green upon its completion. The ‘Progress’ gauge
203 will show the progress of the image processing on a percentage basis. A text file containing
204 results from all the functions can be generated by clicking ‘Save’. The user can specify the path
205 and file name of the text file in a pop-up dialog window.

206

207 **Execution on high performance computing (HPC) clusters**

208 *Execution and code generation on HPC clusters*

209 For executing jobs on HPC clusters, *slurm* (Yoo *et al.*, 2003) is used to submit a batch job, which
210 distributes the jobs using job identifications (IDs). Each job requires a small number of
211 resources, so the priority of execution of each job using *slurm* is high. Thus, owing to less
212 queuing time, we chose *slurm* for *PhenoImage*.

213 Further, to process images using HPC clusters, click the ‘Code’ button (Fig. 2), which
214 generates a MATLAB script for processing images. A *slurm* file (an example is included in
215 *PhenoImage*) is used to submit a job array to the cluster. Then, the job IDs and job size executed
216 by *slurm* are used to partition the images so that each node processes only a part of images. The
217 job IDs and job size are passed to the MATLAB script generated by *PhenoImage* as input
218 parameters. The user needs to input the names of the files that need to be processed in a text file.
219 For each node in the HPC cluster, the script reads all the filenames and processes a part of the
220 images as specified by job ID and job size. Specifically, the script will process images with
221 indices [JobID, JobID+JobSize, JobID+2* JobSize, ...]. The script contains the position of the
222 ROI, the expression of the color filter, and the names of the functions that have been selected for
223 digital trait extraction.

224 After submission of the job using the *slurm* file, the result computed by each function on
225 each node will be printed out and finally aggregated in one output file, which is specified in the
226 *slurm* file. The output file contains all the results for all the input images.

227

228 **Sorghum and wheat: a test case for *PhenoImage* validation**

229 *Sorghum*: Four seeds of sorghum genotype, RTX430 were sown in each of the ten 5.6 liter (L)
230 pots (22 cm diameter X 19.5 cm height) filled with 2.5 kg of a soil mix consisting of 2/3 peat
231 moss and 1/3 vermiculite and 1.4 kg lime. Six days after germination, plants were thinned to one
232 seedling per pot. For the first 21 days, all pots were watered to 70% water holding capacity
233 (WHC). Afterwards, water was withheld from half of the pots (water-limited treatment; WL)
234 until 30% WHC is attained, while half of the pots were maintained at 70% WHC (well-watered
235 treatment; WW; (Supplementary Fig. S1). During the entire experiment, the greenhouse was
236 maintained at 28/25°C temperature, 13h/11h – day/night, and 40-50% relative humidity.

237

238 *Wheat*: Seeds of wheat genotype – Pavon were germinated in Petri dishes for four days in dark at
239 25°C. Uniformly germinated seeds were transplanted in 3 L pots (12 cm diameter X 19.5 cm
240 height) filled with 1.2 kg of Fafard germination soil (Sungro, Massachusetts, USA)
241 supplemented with Osmocote fertilizer and Micromax micronutrients. Seedlings were grown for
242 7 days at 80% WHC. After seven days, 6 seedlings each were maintained at 80% WHC for well-
243 watered treatment and 30% WHC for water-limited treatment (Supplementary Fig. S1). Growth
244 conditions were maintained at 22/16°C – 16/8 h day/night temperatures. Afterwards, plants were
245 imaged every day for 15 days.

246

247 *Water holding capacity (WHC)*

248 For calculating WHC of the soil mix, 2.5 and 1.2 kg of soil mix for sorghum and wheat
249 experiment, respectively, was oven-dried (60°C for 7 days) and dry soil weight was measured.
250 Then, the soil mix was transferred to pots perforated at the bottom for drainage. To achieve the
251 saturation point (weight of the soil at 100% WHC), the soil mix was saturated with water while
252 covered at the top to prevent evaporation. Pots were weighed daily until no change in pot weight
253 was observed. These computed values were then used to calculate the weight of soil at a
254 particular WHC by using the following equation:

Soil weight at a particular WHC

$$= [(Soil\ weight\ at\ 100\%\ WHC - Dry\ Soil\ Weight) \times Required\ WHC] + Dry\ Soil\ Weight$$

255

256 *Plant Imaging*

257 A high-throughput phenotyping facility (LemnaTec Imaging System) at Nebraska Innovation
258 Campus, the University of Nebraska-Lincoln was used to evaluate sorghum (RTx430) and wheat
259 (Pavon) plants by RGB and fluorescence images. For sorghum plants, starting from the day
260 water was withheld, both WW and WL pots were imaged every day until WL pots reached 30%
261 WHC. Plants were imaged for 18 days (Supplementary Fig. S1). Due to technical error during
262 the experiment, the imaging system failed to acquire images on the 13th day of imaging, so data
263 corresponding to this day is missing from the downstream analysis. For wheat plants, imaging
264 was performed for 15 days for WW and WL conditions (Supplementary Fig. S1).

265 To reduce image occlusions, imaging was done from five different angles (side views at
266 0°, 72°, 144°, 216°, and 288°; Supplementary Fig. S2) (Golzarian *et al.*, 2011). Next, RGB and
267 fluorescence images from both the species were used as a test cases to validate *PhenoImage*. For
268 validation and optimal segmentation of RGB images, the following filter parameters were used:
269 $g < 150$ (for sorghum) and $g < 150 \ \& \ h > 0.2 \ \& \ h < 0.5 \ \& \ s > 0.1 \ \& \ v < 0.6 \ \& \ a < -5$ (for wheat).

270 For fluorescence images, plants were imaged in a separate chamber and an ad hoc-image
271 segmentation strategy was used to categorize image color ranges into 32 color classes (Campbell
272 *et al.*, 2015). Further, Hierarchical Cluster Analysis (HCA) was performed using wards method
273 (JMP® Pro13) to examine the temporal profile of the color classes with pixel intensities. For
274 fluorescence images, filters were defined using only the red pixels; sorghum – $r > 150$ and wheat –
275 $r > 50 \ \& \ r < 140$.

276

277 **Performance testing**

278 To test the performance of *PhenoImage*, we evaluated the time required to process images with
279 respect to individual functions such as convex area and pixel count (Supplementary Table S1).
280 For this, an RGB image from a sorghum plant was analyzed at resolutions ranging from 100x100
281 to 10,000x10,000 pixels in an incremental manner.

282

283 **Manual phenotyping and comparisons with other methods**

284 Manual measurements were performed for both sorghum and wheat plants on the last day of
285 imaging in a destructive manner. For this, fresh and dry shoots were weighed. Shoots were dried
286 for one week in an oven at 60°C and weighed to determine the dry weight. The manually derived
287 traits were correlated with digital traits derived from last day of imaging for sorghum and wheat

288 (day 18 and 15, respectively; Supplementary Fig. 1). The RGB images from the last day of
289 imaging were processed using *PhenoImage* (Supplementary Table S2) as well as HTPPheno
290 (Hartmann *et al.*, 2011) and OpenCV (Bradski, 2000) (Supplementary Table S3). For correlation,
291 pixel count derived from *PhenoImage* and OpenCV, and object area from HTPPheno were
292 considered.

293

294 **Results and Discussion**

295 **Performance Testing**

296 We evaluated the performance of *PhenoImage* with respect to the time required to process
297 images. For this, we computed time required to generate data for two functions: convex area and
298 pixel count, derived from RGB images, which had different levels of resolution ranging from
299 100x100 to 10,000x10,000 pixels (Supplementary Table S1). We observed that the application's
300 performance at different resolutions depended on the function that is being evaluated (Fig. 5).
301 For example, time taken to analyze convex area at the highest resolution (10,000x10,000 pixels;
302 1.646 sec) increased by 53.15% compared to the lowest resolution (100x100 pixels; 0.030 sec).
303 On the other hand, time taken to analyze pixel count increased by 16.20% with the increase in
304 the resolution i.e. 0.167 and 0.009 sec for the highest and lowest resolution, respectively (Fig. 5,
305 Supplementary Table S1).

306

307 **Sorghum and wheat: A test case for *PhenoImage* validation**

308 The RGB images from sorghum (RTx430) and wheat (Pavon) were used for validating
309 *PhenoImage*. These species were selected because of their visibly different physical attributes.
310 Sorghum has one main shoot axis, which results in a relatively compact-looking phenotype
311 compared to the wheat plant, which produces multiple tillers (Fig. 5). The two species also differ
312 in other parameters such as stalk diameter, leaf width, leaf length, etc. Plants from both the
313 species were used for HTP with the LemnaTec Imaging System, and images were processed
314 using *PhenoImage*. After loading the images onto the application, the best filter parameters were
315 determined empirically based on histogram generated after segmenting the foreground (i.e. plant
316 pixels) from the background.

317 We assessed two digital traits derived from the RGB images: pixel count and convex
318 area, which are representative of a plant's overall architecture. Pixel count was used as a proxy

319 for projected shoot area (PSA) and represents the total number of pixels of a plant, whereas the
320 convex area was the area of the convex hull and illustrates the smallest convex polygon
321 enclosing all of the pixels of the plant (Fig. 3). For validation, the visible differences between the
322 two species were assessed for plants of the same age (26-day old) via imaging. As a result, we
323 detected significant differences ($P < 0.001$) between sorghum and wheat plants with respect to
324 PSA as well as the convex area (Fig. 6). Interestingly, although wheat plants have a higher
325 number of leaves than sorghum of the same age, sorghum plants had higher PSA and convex
326 area, apparently due to the broader leaves of sorghum.

327

328 **Comparison with manual measurements and other image processing methodologies**

329 Next, we performed destructive phenotyping of sorghum and wheat plants at the last day of
330 imaging (day 18 and 15, respectively; Supplementary Fig. S1). The harvested plants were used to
331 manually record fresh and dry shoot weight. As expected, we observed significantly higher fresh
332 and dry weight for sorghum compared to wheat (Supplementary Table S2).

333 Furthermore, we compared the manually recorded phenotypes with digital traits (pixel
334 count) derived from RGB images. For this, the RGB images were processed using the in-house
335 generated application – *PhenoImage*, as well as two publicly available tools, HTPPheno and
336 OpenCV. HTPPheno is used as a plugin for ImageJ and does not involve programming language
337 (Hartmann *et al.*, 2011). The application does not allow calibration of color settings for image
338 processing. On the other hand, OpenCV requires skills in Python programming language and
339 does not offer GUI (Bradski, 2000). For both the plant species, we detected a high correlation for
340 fresh and dry weight with PSA derived from RGB images processed using *PhenoImage*, which
341 was comparable to correlations obtained from HTPPheno and OpenCV (Table 1 and
342 Supplementary Table S2 and S3). This illustrates the sensitivity of the *PhenoImage* application
343 in terms of estimating digital traits from the two plant species while considering minute details in
344 depth.

345

346 **Temporal analysis of growth dynamics using *PhenoImage***

347 The image-based phenotyping platforms have enabled quantification of physiological and
348 morphological features in a time-dependent manner. In this context, we performed temporal
349 evaluation of sorghum and wheat growth dynamics under well-watered (WW) and water-limited

350 (WL) conditions using HTP. The RGB and fluorescent derived images were processed using
351 *PhenoImage* for testing sensitivity of the tool to detect subtle physiological changes over time.

352 The biomass of the plant increases with growth and development, which can be
353 quantified by imaging, and environmental stresses in general slow growth and development
354 (Chen *et al.*, 2014; Röth *et al.*, 2016). To evaluate the changes in plant size in a temporal manner,
355 we traced PSA derived from RGB images under WW and WL conditions. For both sorghum and
356 wheat, PSA showed a gradual increase over time under WW and WL; however, WL conditions
357 exhibited lower PSA relative to WW conditions for the identical time-point (Fig. 7).

358 We evaluated changes in pixel intensities corresponding to the ‘G’ channel and
359 chlorophyll fluorescence as an indicator of plant health. In principle, the ‘G’ pixel intensity
360 derived from the RGB images reflect the greenness of the plant; higher green pixel intensity
361 reflects higher chlorophyll content, which in turn is associated with the higher photosynthetic
362 activity (Wood *et al.*, 2020). The greenness index (GI) was calculated using the following
363 formula: $I = \frac{N_G}{N_R + N_G + N_B}$, where N_R , N_G , and N_B are pixel intensity for R, G, and B channel
364 normalized to total pixel count for the respective time-point and treatment. For both sorghum and
365 wheat, we observed higher GI under WW relative to WL conditions (Fig. 8).

366 Furthermore, abiotic stresses such as heat stress or water limitation decreases
367 photosynthetic efficiency and increases non-photochemical quenching resulting in enhanced
368 chlorophyll fluorescence and heat dissipation (Zhao *et al.*, 2017; Paul *et al.*, 2020). Therefore, we
369 evaluated the dynamics of chlorophyll fluorescence for sorghum and wheat under WW and WL
370 conditions. For this, total pixels corresponding to the red channel were classified into 32 color
371 classes based on their fluorescence intensity. As the stress progressed, fluorescent intensity of
372 pixels changed. To monitor the rearrangement of pixels over time and treatments, we performed
373 HCA. As a result, we detected four clusters (I-IV) each for sorghum and wheat (Fig. 9; left
374 panel). For sorghum, the identified clusters distinguished changes related to both development as
375 well as water treatments (WW and WL). Cluster I comprised fluorescence changes at early time
376 points – 1 to 5 day (d) of imaging, wherein cluster II and III were associated with later time
377 points (d6 to d17) under both WW and WL conditions (Fig. 9). Furthermore, HCA clearly
378 distinguished fluorescence changes linked with water treatment, as cluster II and III were
379 predominant ones under WL and WW conditions, respectively (Fig. 9). In the case of wheat,
380 HCA distinguished development-driven fluorescence changes, as early time points (d1 to d5)

381 were represented by cluster I and II and late time points (d6 to d15) were represented by cluster
382 III and IV (Fig. 9; right panel). However, a clear distinction between WW and WL conditions
383 was not observed. These results are in line with previous findings documenting decreased
384 chlorophyll content or photosynthetic activity as a possible penalty on a plant subjected to WL
385 conditions (Mathobo *et al.*, 2017).

386 Collectively, the results establish that *PhenoImage* can be used to analyze HTP-derived
387 longitudinal phenotypic datasets (RGB and fluorescence images) to detect the occurrence of
388 subtle phenotypic changes in a plant's growth and development.

389

390 **Conclusion**

391 *PhenoImage* offers an exhaustive and robust analysis of large-scale plant phenotyping data. The
392 intuitiveness of the application allows scientists with little programming experience to process
393 large-scale datasets on their computers. The tool can also support parallel high performance
394 computing clusters. The availability of multiple functions and filtering parameters provides
395 flexibility to analyze a wide variety of plant species. Moreover, open-source nature provides the
396 possibility to extend the usability of the tool to meet specific user requirements. The current
397 version of the application is designed for analyzing aboveground plant images. However, we
398 plan to extend its usability to examine other tissues such as root or panicles.

399

400 **Author Contributions**

401 HW, HY, SS, and PS supervised the project. PP led the study. FZ designed and developed the
402 application. MS and JS performed the experiment. MS, JS, and PP analyzed the results. PP wrote
403 the manuscript with inputs from MS, JS, and FZ. All authors read and approve the manuscript.

404

405 **Funding**

406 This work was supported by National Science Foundation Award # 1736192 to HW and HY, and
407 by a gift from Kamterter Products, LLC, Waverly, Nebraska to PS.

408

409 **Acknowledgements**

410 We would like to thank the Nebraska Innovation Campus, University of Nebraska, Lincoln, USA
411 for their support for the imaging experiments.

412

413 **Software Availability**

414 *PhenoImage* is available in two different versions: (i) Standalone application: this version does
415 not require MATLAB license for its operation, (ii) Regular application: this version does require
416 MATLAB: <https://www.mathworks.com/products/matlab.html>.

417 Both versions are available at <http://wrchr.org/phenolib/phenoimage>. We have provided a
418 detailed step-by-step guide for using *PhenoImage* (*PhenoImage* Guide Document).

419

420

Table 1: Correlation of manual traits – fresh weight (FW) and dry weight (DW) with the digital trait derived from RGB images processed using the three applications.

	<i>PhenoImage</i>	HTPheno	OpenCV
FW (Sorghum)	0.923	0.897	0.901
FW (Wheat)	0.927	0.999	0.901
DW (Sorghum)	0.974	0.960	0.962
DW (Wheat)	0.863	0.871	0.999

For comparisons, pixel count derived from *PhenoImage* and OpenCV, and object area from HTPheno for both plant species corresponding to the last day of imaging were used.

421

422 **Supplementary Material**

423 Supplementary Fig. S1: Water treatments for sorghum and wheat. For sorghum, all pots were
424 watered to 70% water holding capacity (WHC) for the first 21 days. Then, water was withheld
425 from half of the pots (water-limited treatment; WL) until 30% WHC is attained, while half of the
426 pots were maintained at 70%WHC (well-watered treatment; WW). During the entire experiment,
427 the greenhouse was maintained at 28/25°C temperature, 13h/11h – day/night, and 40-50%
428 relative humidity. For wheat, seedlings were grown for 7 days at 80% WHC. After seven days,
429 half of the seedlings were maintained at 80% WHC for WW treatment. For the other half, water
430 was withheld until 30% WHC is attained (WL treatment). Growth conditions were maintained at
431 22/16°C – 16/8 h day/night temperatures. Afterwards, plants were imaged every day for 15 days.

432

433 Supplementary Fig. S2: Representative RGB original and processed images of sorghum and
434 wheat plants from five different angles.

435

436 Supplementary Table S1: To test the performance of *PhenoImage*, we evaluated the time
437 required to process images with respect to individual functions: convex area and pixel count. For
438 this, an RGB image from a sorghum plant was analyzed at resolutions ranging from 100x100 to
439 10,000x10,000 pixels in an incremental manner.

440

441 Supplementary Table S2: Sorghum and wheat plants from the last day of imaging (day 18 and
442 15, respectively) were harvested for recording manual traits (fresh and dry weight; FW and DW).
443 These manual traits were correlated with digital traits derived from RGB images processed using
444 PhenoImage. $n = 5$ and 6 for sorghum and wheat, respectively.

445

446 Supplementary Table S3: Sorghum and wheat plants from the last day of imaging (day 18 and
447 15, respectively) were harvested for recording manual traits (fresh and dry weight; FW and DW).
448 These manual traits were correlated with digital traits derived from RGB images processed using
449 PhenoImage and OpenCV (Pixel count), and HTPPheno (Object Area).

450

451 **Figure Legends:**

452 Fig. 1. *PhenoImage* Workflow. First, the path of the folder containing RGB images is described.
453 Then, a region of interest containing plant image is defined, followed by the selection of color
454 space of preference. Afterwards, filter parameters are determined, and functions corresponding to
455 the digital traits of users' choice are selected. Then, the processing of the images is executed
456 using either a local CPU or high-performance computing clusters.

457
458 Fig. 2. Graphical user interface (GUI) of *PhenoImage*. The numbers denote a step-by-step guide
459 to use the application: (1) define '*Path*' of the folder containing plant images and click '*Load*'
460 button, (2) '*Light bulb*' shows status of the loading procedure, as the blue '*Light bulb*' turns red
461 while the loading is in progress and green when completed, (3) one of the image from the folder
462 is displayed in the '*Original Image*' section, (4) the spinner can be used to change the current
463 image shown in the '*Original Image*' space, (5) then, the user must define '*Region of interest*' or
464 '*ROI*' by dragging the cursor on the *Original image*, (6) select the '*Color space*' of preference,
465 (7 and 8) click on '*Histogram*' button to visualize intensity of channels corresponding to the
466 respective '*Color space*', (9a and b) the user can either directly use the histogram values to
467 define the '*Filter*' or the user can use the '*Segmentation*' function, where '*Foreground*' and
468 '*Background*' need to be specified to precisely segment plant pixels from the background, (10
469 and 11) the user can click '*Test*' to view the '*Processed image*' and if the user has decided on the
470 '*Filter*' (12) then, selection of '*Functions*' is performed. The functions or the digital parameters
471 that need to be extracted are based on user preference. (13) If running on a single machine, the
472 user can '*Execute*' the function to process all images in the respective folder, and progress of
473 batch processing can be viewed in the '*Progress bar*' and saved or (14) high-performance
474 computing clusters can be used to process the images.

475
476 Fig. 3. Representation of different features used by *PhenoImage*. The cropped image is derived
477 from the original image after the selection of the region of interest. The binary image is a mask
478 of the plant pixels where the plant pixels are set to 1 and the background is set to 0. The
479 segmented image represents the segmented plant pixels from the background. The bounding box
480 shown in the light blue color is calculated based on the segmented pixels and encloses all pixels
481 of the plant. Convex hull signifies the smallest convex polygon enclosing all the pixels of the

482 plant. The image skeleton approximates the center lines of the stem and the leaves and is
483 calculated using a skeletonization algorithm.

484

485 Fig. 4. Segmentation. For subtracting plant pixels from the background, click on ‘*Foreground*’
486 and new a pop-up window displaying the original image opens. The user can scribble on the area
487 of interest with a red mark. Likewise, the user can define background (i.e. pot, pot stand, plant
488 background, etc.) by scribbling on the background using a green mark. Afterwards, the user can
489 click the ‘*Segment*’ button to initiate the segmentation of plant pixels from the background. As a
490 result, the ‘*Processed Image*’ will show pixels corresponding only to the plant.

491

492 Fig. 5. Performance testing of *PhenoImage*. The plot shows the time taken to process images and
493 extract the respective digital trait (convex area and pixel count) from the images at different
494 resolution.

495

496 Fig. 6. *PhenoImage* validation. (A) The RGB images from 26-day old sorghum and wheat plants.
497 Two digital traits: convex area and projected shoot area (PSA), which represent a plant’s
498 architecture were derived using *PhenoImage*. Significant differences ($P < 0.001$) were detected
499 between sorghum ($n = 5$) and wheat ($n = 6$) for both the digital traits. For statistics, Welch’s t -
500 test (equal variance not assumed) was used.

501

502 Fig. 7. Temporal analysis of growth dynamics. Sorghum and wheat plants subjected to well-
503 watered (WW) and water-limited (WL) conditions were imaged in a time-dependent manner
504 using the LemnaTec Imaging System. Sorghum and wheat plants were imaged for 18 and 15
505 days, respectively. *PhenoImage* derived projected shoot area (PSA) showed significant
506 differences between WW and WL conditions on the 8th day for both sorghum ($n = 5$) and wheat
507 ($n = 6$). For statistics, the paired t -test was used. The grey box represents the significance
508 difference between WW and WL treatments for the respective days.

509

510 Fig. 8. The heat map exhibits the ‘Greenness Index’ for sorghum and wheat under well-watered
511 (WW) and water-limited (WL) conditions in a time-dependent manner.

512

513 Fig. 9. Hierarchical Cluster Analysis of fluorescence color classes for sorghum (left panel) and
514 wheat (right panel). Normalized pixel counts corresponding to different color classes were
515 clustered (I to IV) using wards method in JMP® Pro13 under well-watered (WW) and water-
516 limited (WL) conditions. Days of imaging under WW and WL treated plants were represented by
517 blue and red-colored numerals, respectively.

518 **References:**

- 519 **Abeysinghe SS, Baker M, Chiu W, Ju T.** 2008. Segmentation-free skeletonization of grayscale
520 volumes for shape understanding. IEEE International Conference on Shape Modeling and
521 Applications 2008, Proceedings, SMI.63–71.
- 522 **Bradski G.** 2000. The OpenCV Library. Doctor Dobbs Journal **25**, 120–126.
- 523 **Campbell MT, Knecht AC, Berger B, Brien CJ, Wang D, Walia H.** 2015. Integrating image-
524 based phenomics and association analysis to dissect the genetic architecture of temporal salinity
525 responses in rice. Plant Physiology **168**, 1476–1489.
- 526 **Chen D, Neumann K, Friedel S, Kilian B, Chen M, Altmann T, Klukas C.** 2014. Dissecting
527 the phenotypic components of crop plant growthand drought responses based on high-throughput
528 image analysis w open. Plant Cell **26**, 4636–4655.
- 529 **Fahlgren N, Gehan MA, Baxter I.** 2015. Lights, camera, action: high-throughput plant
530 phenotyping is ready for a close-up. Current Opinion in Plant Biology **24**, 93–99.
- 531 **Fiorani F, Schurr U.** 2013. Future Scenarios for Plant Phenotyping. Annual Review of Plant
532 Biology **64**, 267–291.
- 533 **Furbank RT, Tester M.** 2011. Phenomics - technologies to relieve the phenotyping bottleneck.
534 Trends in Plant Science **16**, 635–644.
- 535 **Gehan MA, Fahlgren N, Abbasi A, et al.** 2017. PlantCV v2: Image analysis software for high-
536 throughput plant phenotyping. PeerJ **2017**, 1–23.
- 537 **Golzarian MR, Frick RA, Rajendran K, Berger B, Roy S, Tester M, Lun DS.** 2011.
538 Accurate inference of shoot biomass from high-throughput images of cereal plants. Plant
539 Methods **7**, 2.
- 540 **Gong P, He C.** 2014. Uncovering Divergence of Rice Exon Junction Complex Core
541 Heterodimer Gene Duplication Reveals Their Essential Role in Growth, Development, and
542 Reproduction. Plant Physiology **165**, 1047–1061.
- 543 **Hartmann A, Czauderna T, Hoffmann R, Stein N, Schreiber F.** 2011. HTPPheno: An image
544 analysis pipeline for high-throughput plant phenotyping. BMC Bioinformatics **12**, 148.
- 545 **Houle D, Govindaraju DR, Omholt S.** 2010. Phenomics: The next challenge. Nature Reviews
546 Genetics **11**, 855–866.
- 547 **Hu MK.** 1962. Visual Pattern Recognition by Moment Invariants. IRE Transactions on
548 Information Theory **8**, 179–187.
- 549 **Jackson SA, Iwata A, Lee S-H, Schmutz J, Shoemaker R.** 2011. Sequencing crop genomes:
550 approaches and applications. New Phytologist **191**, 915–925.
- 551 **Klukas C, Chen D, Pape JM.** 2014. Integrated analysis platform: An open-source information
552 system for high-throughput plant phenotyping. Plant Physiology **165**, 506–518.
- 553 **Knecht AC, Campbell MT, Caprez A, Swanson DR, Walia H.** 2016. Image Harvest: An
554 open-source platform for high-throughput plant image processing and analysis. Journal of
555 Experimental Botany **67**, 3587–3599.
- 556 **Li L, Zhang Q, Huang D, Li L, Zhang Q, Huang D.** 2014. A review of imaging techniques for
557 plant phenotyping. Sensors **14**, 20078–20111.
- 558 **Lobet G, Draye X, Périlleux C.** 2013. An online database for plant image analysis software
559 tools. Plant Methods **9**, 38
- 560 **Mathobo R, Marais D, Steyn JM.** 2017. The effect of drought stress on yield, leaf gaseous
561 exchange and chlorophyll fluorescence of dry beans (*Phaseolus vulgaris* L.). Agricultural Water
562 Management **180**, 118–125.
- 563 **Minervini M, Schar H, Tsiftaris SA.** 2015. Image analysis: The new bottleneck in plant

564 phenotyping [applications corner]. *IEEE Signal Processing Magazine* **32**, 126–131.
565 **Moose SP, Mumm RH.** 2008. Molecular plant breeding as the foundation for 21st century crop
566 improvement. *Plant Physiology* **147**, 969–977.
567 **Paul P, Mesihovic A, Chaturvedi P, Ghatak A, Weckwerth W, Böhmer M, Schleiff E.** 2020.
568 Structural and functional heat stress responses of chloroplasts of *Arabidopsis thaliana*. *Genes* **11**,
569 1–20.
570 **Röth S, Paul P, Fragkostefanakis S.** 2016. Plant heat stress response and thermotolerance. In: Jaiwal P.,
571 Singh R., Dhankher O. (eds) *Genetic Manipulation in Plants for Mitigation of Climate Change*. Springer,
572 New Delhi.
573 **Tester M, Langridge P.** 2010. Breeding technologies to increase crop production in a changing
574 world. *Science* **327**, 818–822.
575 **Varshney RK, Nayak SN, May GD, Jackson SA.** 2009. Next-generation sequencing
576 technologies and their implications for crop genetics and breeding. *Trends in Biotechnology* **27**,
577 522–530.
578 **Wood NJ, Baker A, Quinnell RJ, Camargo-Valero MA.** 2020. A Simple and Non-destructive
579 Method for Chlorophyll Quantification of *Chlamydomonas* Cultures Using Digital Image
580 Analysis. *Frontiers in Bioengineering and Biotechnology* **8**:746.
581 **Yang W, Feng H, Zhang X, Zhang J, Doonan J.** 2020. Crop phenomics and high-throughput
582 phenotyping: past decades, current challenges, and future perspectives. *Molecular Plant* **13**, 187–
583 214.
584 **Yoo AB, Jette MA, Grondona M.** 2003. SLURM: Simple Linux Utility for Resource
585 Management. *Lecture Notes in Computer Science (including subseries Lecture Notes in*
586 *Artificial Intelligence and Lecture Notes in Bioinformatics)* **2862**, 44–60.
587 **Zhao X, Chen T, Feng B, Zhang C, Peng S, Zhang X, Fu G, Tao L.** 2017. Non-
588 photochemical quenching plays a key role in light acclimation of rice plants differing in leaf
589 color. *Frontiers in Plant Science* **7**, 1968.
590 **Zhu F, Paul P, Hussain W, Wallman K, Dhatt BK, Irvin L, Morota G, Yu H, Walia H.**
591 2020. SeedExtractor: an open-source GUI for seed image analysis. *bioRxiv*, 2020.06.28.176230.
592

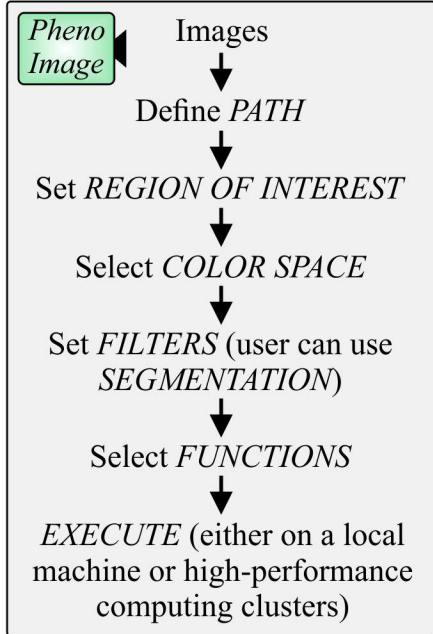


Fig. 1. *PhenoImage* Workflow. First, the path of the folder containing RGB images is described. Then, a region of interest containing plant image is defined, followed by the selection of color space of preference. Afterwards, filter parameters are determined, and functions corresponding to the digital traits of users' choice are selected. Then, the processing of the images is executed using either a local CPU or high-performance computing clusters.

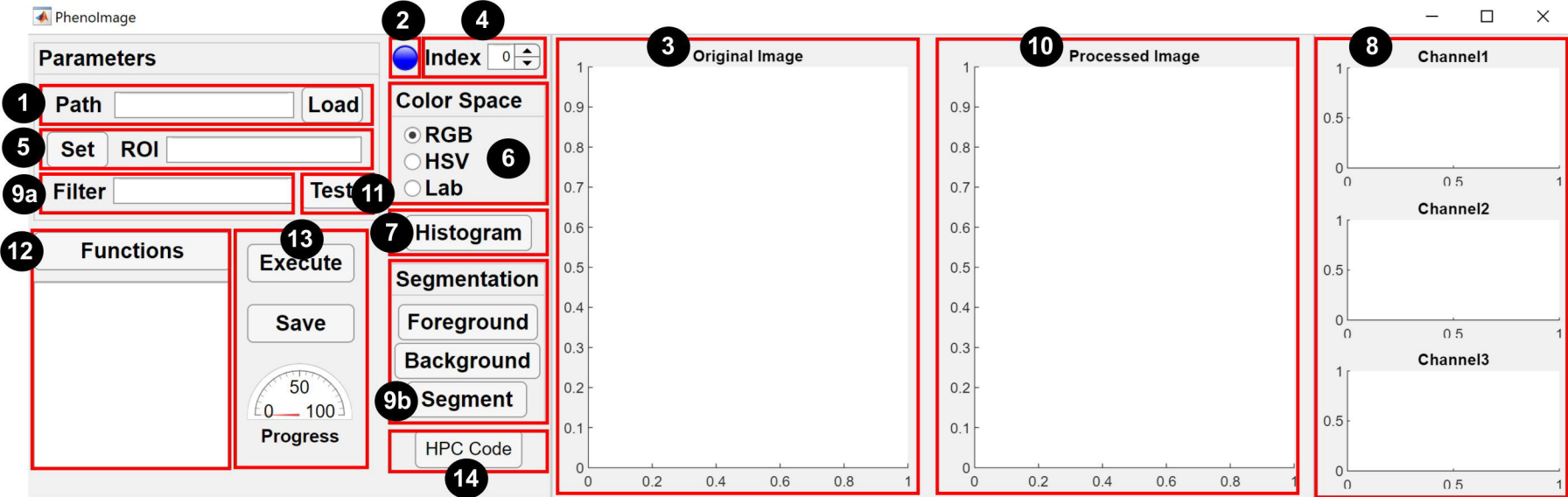


Fig. 2. Graphical user interface (GUI) of *PhenoImage*. The numbers denote a step-by-step guide to use the application: (1) define ‘*Path*’ of the folder containing plant images and click ‘*Load*’ button, (2) ‘*Light bulb*’ shows status of the loading procedure, as the blue ‘*Light bulb*’ turns red while the loading is in progress and green when completed, (3) one of the image from the folder is displayed in the ‘*Original Image*’ section, (4) the spinner can be used to change the current image shown in the ‘*Original Image*’ space, (5) then, the user must define ‘*Region of interest*’ or ‘*ROI*’ by dragging the cursor on the *Original image*, (6) select the ‘*Color space*’ of preference, (7 and 8) click on ‘*Histogram*’ button to visualize intensity of channels corresponding to the respective ‘*Color space*’, (9a and b) the user can either directly use the histogram values to define the ‘*Filter*’ or the user can use the ‘*Segmentation*’ function, where ‘*Foreground*’ and ‘*Background*’ need to be specified to precisely segment plant pixels from the background, (10 and 11) the user can click ‘*Test*’ to view the ‘*Processed image*’ and if the user has decided on the ‘*Filter*’ (12) then, selection of ‘*Functions*’ is performed. The functions or the digital parameters that need to be extracted are based on user preference. (13) If running on a single machine, the user can ‘*Execute*’ the function to process all images in the respective folder, and progress of batch processing can be viewed in the ‘*Progress bar*’ and saved or (14) high-performance computing clusters can be used to process the images.

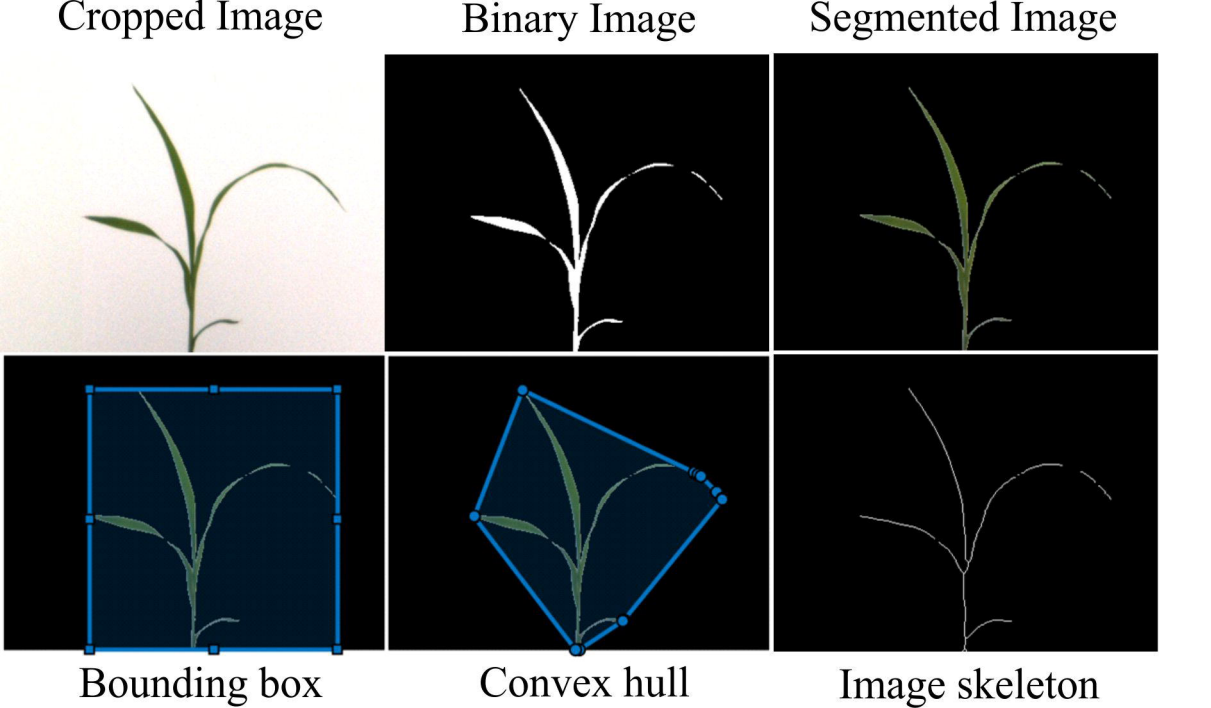
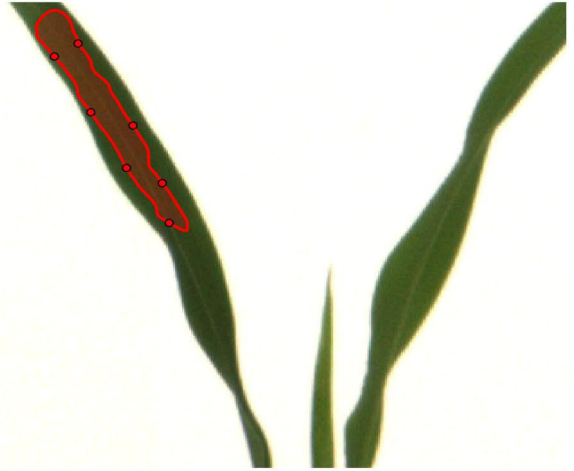


Fig. 3. Representation of different features used by *PhenoImage*. The cropped image is derived from the original image after the selection of the region of interest. The binary image is a mask of the plant pixels where the plant pixels are set to 1 and the background is set to 0. The segmented image represents the segmented plant pixels from the background. The bounding box shown in the light blue color is calculated based on the segmented pixels and encloses all pixels of the plant. Convex hull signifies the smallest convex polygon enclosing all the pixels of the plant. The image skeleton approximates the center lines of the stem and the leaves and is calculated using a skeletonization algorithm.

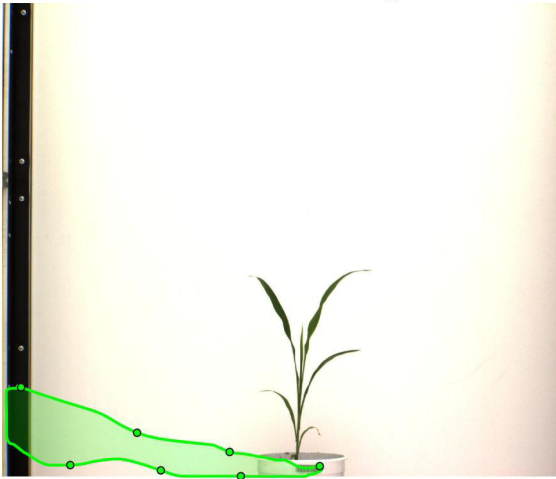
Original Image



Selection of Foreground



Selection of Background



Processed Image

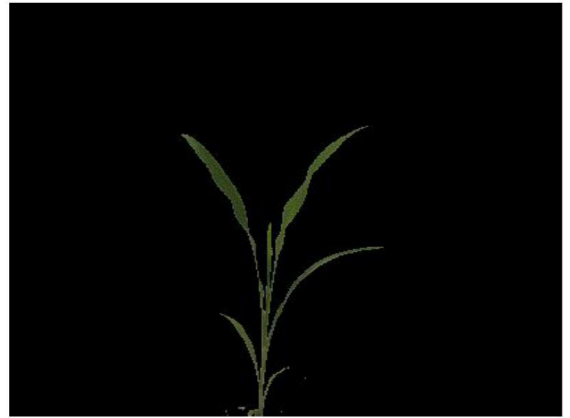


Fig. 4. Segmentation. For subtracting plant pixels from the background, click on ‘*Foreground*’ and new a pop-up window displaying the original image opens. The user can scribble on the area of interest with a red mark. Likewise, the user can define background (i.e. pot, pot stand, plant background, etc.) by scribbling on the background using a green mark. Afterwards, the user can click the ‘*Segment*’ button to initiate the segmentation of plant pixels from the background. As a result, the ‘*Processed Image*’ will show pixels corresponding only to the plant.

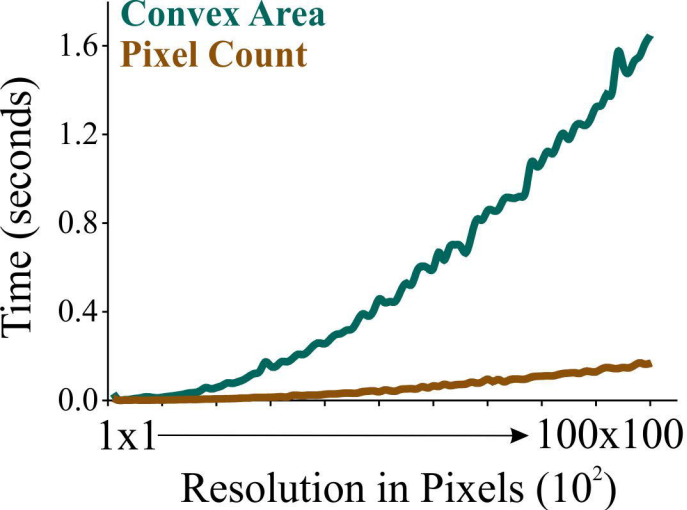
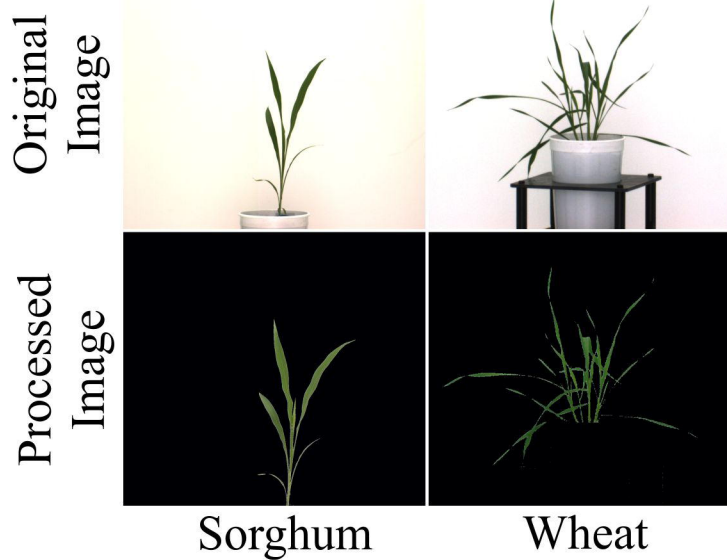


Fig. 5. Performance testing of *PhenoImage*. The plot shows the time taken to process images and extract the respective digital trait (convex area and pixel count) from the images at different resolution.

A

26-days old plants



B

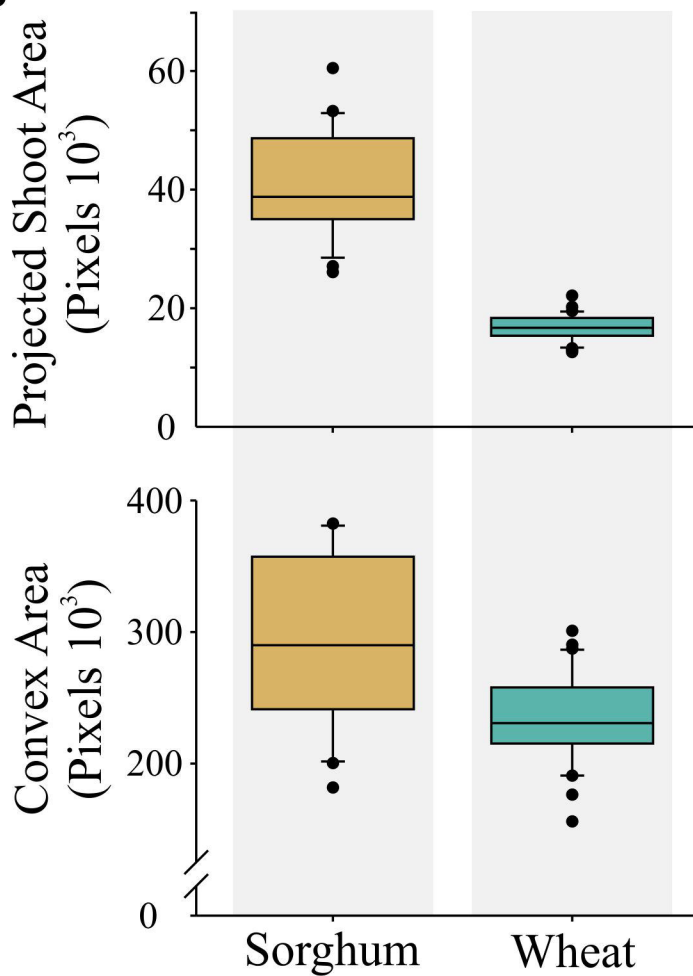


Fig. 6. *PhenoImage* validation. (A) The RGB images from 26-day old sorghum and wheat plants. Two digital traits: convex area and projected shoot area (PSA), which represent a plant's architecture were derived using *PhenoImage*. Significant differences ($P < 0.001$) were detected between sorghum ($n = 5$) and wheat ($n = 6$) for both the digital traits. For statistics, Welch's t-test (equal variance not assumed) was used.

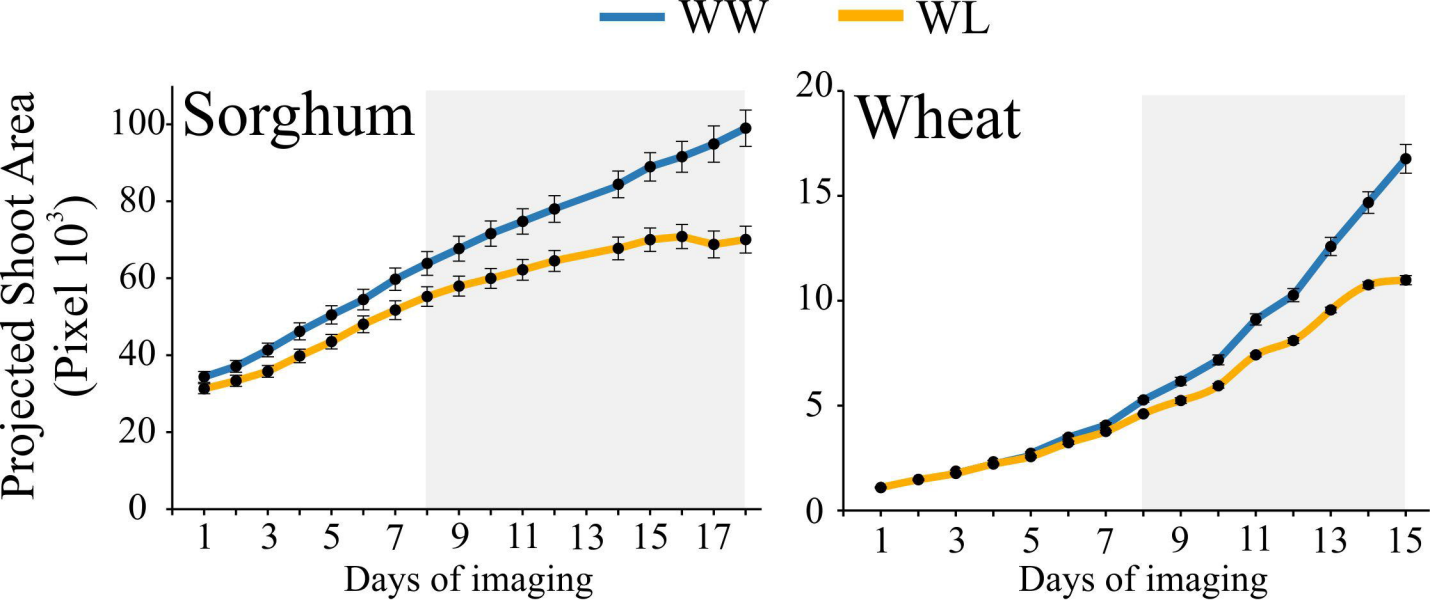


Fig. 7. Temporal analysis of growth dynamics. Sorghum and wheat plants subjected to well-watered (WW) and water-limited (WL) conditions were imaged in a time-dependent manner using the LemnaTec Imaging System. Sorghum and wheat plants were imaged for 18 and 15 days, respectively. *PhenoImage* derived projected shoot area (PSA) showed significant differences between WW and WL conditions on the 8th day for both sorghum ($n = 5$) and wheat ($n = 6$). For statistics, the paired t -test was used. The grey box represents the significance difference between WW and WL treatments for the respective days.

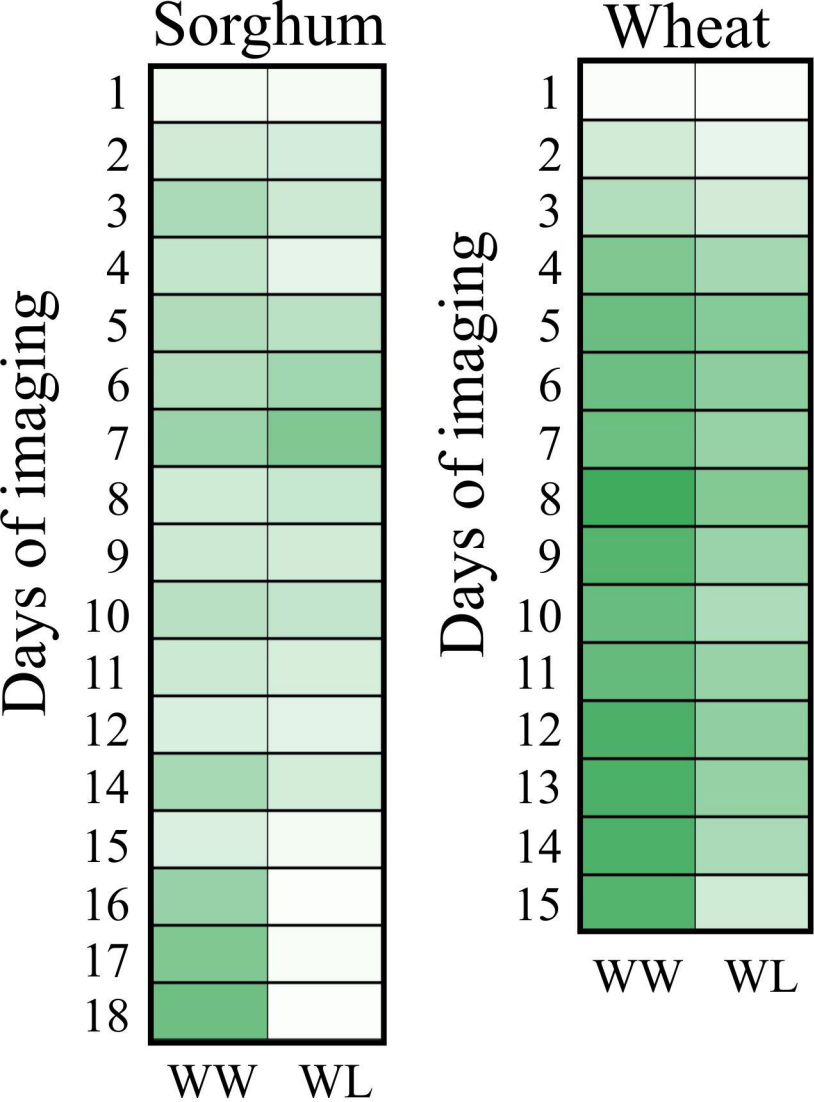


Fig. 8. The heat map exhibits the 'Greenness Index' for sorghum and wheat under well-watered (WW) and water-limited (WL) conditions in a time-dependent manner.

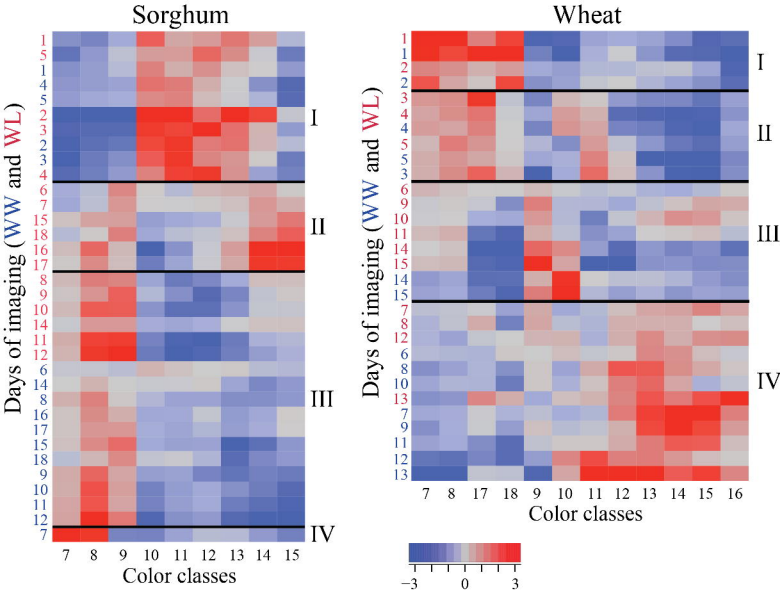


Fig. 9. Hierarchical Cluster Analysis of fluorescence color classes for sorghum (left panel) and wheat (right panel). Normalized pixel counts corresponding to different color classes were clustered (I to IV) using Wards method in JMP Pro 13 under well-watered (WW) and water-limited (WL) conditions. Days of imaging under WW and WL treated plants were represented by blue and red colored numerals, respectively.